Fatigue Behavior of Swept Spot Friction Welds in Lap-Shear Specimens of Alclad 2024-T3 Aluminum Sheets

Z.M. Su [1], R.Y. He[1], P.C. Lin[1], J.N. Aoh[1], Y.C. Chiou[2], M.T. Dong[3], T. Tang[3] and B. Huang[3]*

1.National Chung Cheng University and Advanced Institute for Manufacturing with High-tech Innovations

2. National Chiayi University

3.Aerospace Industrial Development Corporation

imepcl@ccu.edu.tw

Abstract-Failure modes of swept spot friction welds in lap-shear specimens of alclad 2024-T3 aluminum sheets are first investigated based on experimental observations. Optical and scanning electron micrographs of the welds before and after failure under quasi-static and cyclic loading conditions are examined. Experimental results show that the failure modes of the welds under quasi-static and cyclic loading conditions are quite different. Under quasi-static loading conditions, the failure mainly starts from the necking of the upper sheet near the boundary of the stir zone. Under low-cycle loading conditions, the dominant fatigue crack is the kinked crack growing into the upper sheet from the crack tip; hence, the upper nugget pullout failure mode can be seen. Under higher load ranges of high-cycle loading conditions, the dominant kinked fatigue crack grows into the lower sheet from the surface of the curved interface; subsequently, a separation of the lower sheet can be seen. Finally, under lower load ranges of high-cycle loading conditions, the dominant kinked fatigue crack grows into the upper sheet from the crack tips. Then, a separation of the upper sheet can be seen. In summary, failure modes of swept spot friction welds strongly depend on the weld geometry, microstructure, and load amplitude.

Keywords - Spot friction weld, friction stir spot weld, Alclad, 2024-T3, fatigue

I. INTRODUCTION

Resistance spot welding is the most commonly used joining technique for body-in-white parts made of steel sheets. However, resistance spot welding of aluminum sheets is likely to produce poor welds due to numerous voids and defects inside the nugget [1,2]. A spot friction welding (SFW) process was therefore developed by Mazda Motor Corporation and Kawasaki Heavy Industry [3,4]. Importantly, the spot friction welding process makes joints without melting the base metal in contrast with conventional welding processes. Recently, a variation of the "traditional" spot friction welding process was proposed by Buffa et al. [5] and Tweedy et al. [6]. As shown in Fig. 1, the rotating tool is first indented into the sheets. Then the tool is moved rightward for a given path radius and then swept along a circular tool path to stir more material during the process. Finally, the tool move back to the initial indentation site and a swept spot friction weld (or a swept friction stir spot weld) is made. In general, the mechanical performance of the swept spot friction weld is better than that of the "traditional" spot friction weld mainly due to a larger stir zone.

Mechanical performance and microstructure evolution of swept spot friction welds were studied, for example, Buffa et al. [5] and Tweedy et al. [6]. Recently, Brown et al. [7,8] investigated the fatigue performance of swept spot friction welds between similar and dissimilar sheet materials. Aluminum sheets with different surface treatments including alclading, anodizing, and alodining were also considered. Their results showed that the fatigue lives of swept spot friction welds with different surface treatments were slight below those of rivets. However, the fracture and fatigue behaviors of swept spot friction welds, which correlate well to the fatigue life estimation, have not been well investigated in the literature. Therefore, swept spot friction welds in lap-shear specimens of alclad 2024-T3 aluminum sheets were tested under quasi-static and cyclic loading conditions in this investigation.

In this paper, fracture and fatigue behaviors of swept spot friction welds in lap-shear specimens are investigated based on experimental observations. Alclad 2024-T4 aluminum sheets with the thickness of 1.6 mm were used. A tool with a flat shoulder and a triangular probe was used to make the welds investigated here. A circular tool path with a path radius of 1.5 mm is considered. Optical and scanning electron micrographs of the welds before and after failure under quasi-static and cyclic loading conditions are examined. The failure modes of swept spot friction welds under quasi-static, low-cycle and high-cycle fatigue loading conditions are then investigated. Finally, the paths of the dominant kinked fatigue cracks for the welds are identified.

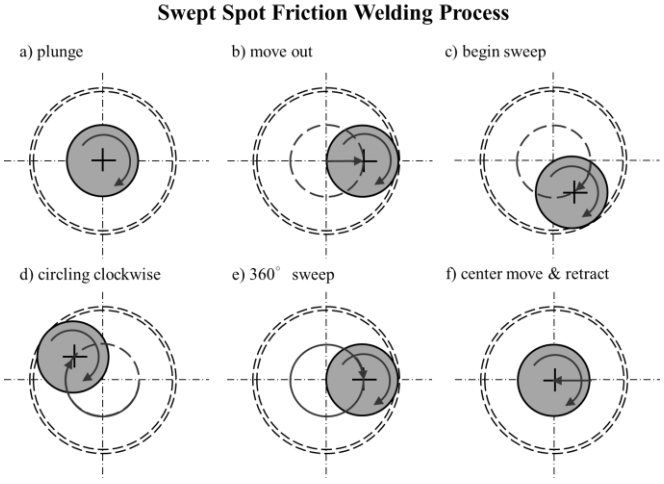

Fig. 1 A schematic of the circular tool path.

II. SWEPT SPOT FRICTION WELDS OF ALCLAD 2024-T3 ALUMINUM SHEETS

Alclad 2024-T3 aluminum sheets with a thickness of 1.6 mm were used for swept spot friction welding. Note that alclading is a corrosion resistance process in which thin pure

aluminum layers are bonded on the surfaces of high-strength aluminum alloy sheets. Here, two aluminum 1230 layers with a thickness of 0.05mm were bonded on each sheet surfaces. A tool with a flat shoulder and a M5 threaded triangular probe was used. The diameter of the tool shoulder is 12 mm. The diameter and length of the probe pin are 5 mm and 2.8 mm, respectively. For the initial indentation, a tool rotational speed of 500 rpm, a tool indentation depth of 2.8 mm, and a tool indentation rate of 120 mm/min were applied. For the following circular tool path, a feed rate of 180 mm/min and a path radius of 1.5 mm were applied. Note that these processing parameters were determined by the design of experiments (DOE) for the maximum failure loads of welds in lap-shear specimens.

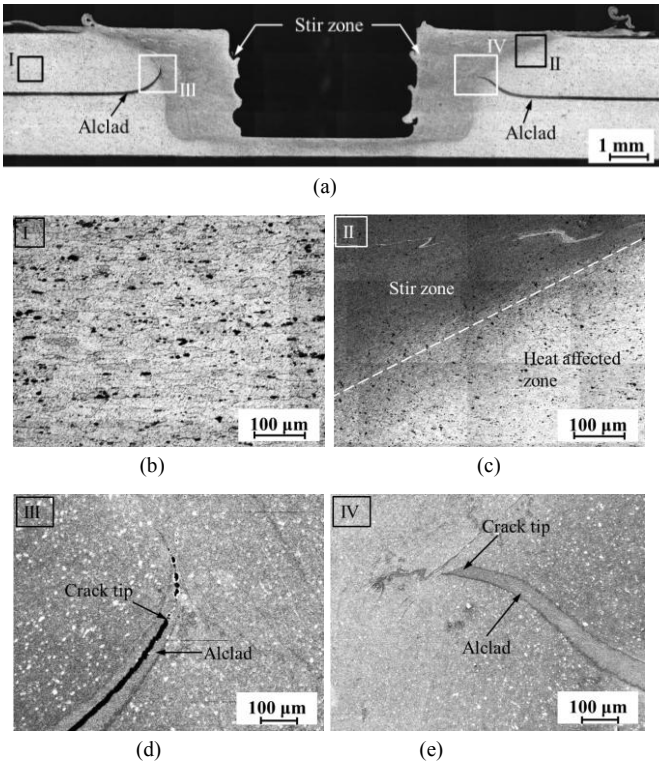

Fig. 2(a) An optical micrograph of the cross section along the symmetry plane of a swept spot friction weld, (b) a close-up optical micrograph of region I, (c) a close-up optical micrograph of region II, (d) a close-up scanning electron micrograph of region III, (e) a close-up scanning electron micrograph of region IV.

Fig. 2(a) shows an optical micrograph of the cross section along the symmetry plane of a swept spot friction weld before testing. As shown in the figure, the indentation profile reflects the general shape of the tool shoulder and probe pin. The tool shoulder and probe pin squeeze out a portion of the upper sheet material and consequently, the squeezed out material forms an annular film on the top surface of the upper sheet along the outer circumference of the shoulder indentation. Near the central hole, the two gray areas near the central hole of welds are denoted as the stir zone where the materials are severely plastically deformed and recrystallized. Note that the pure aluminum layers bonded on the top and bottom surfaces of 2024-T3 sheets are completely stirred and uniformly distributed inside the stir zone mainly due to the circular tool path. Also the stir zone size of the swept spot friction weld appears to be larger than that of the "traditional" spot friction weld in [3]. In Fig. 2(b), a close-up view of region I shows relatively coarse grains in the base metal. In Fig. 2(c), a close-up view of region II shows finer grains in the stir zone. Figs. 2(d) and 2(e) show close-up views of regions III and IV where the curved interfacial surfaces become cracks and gradually disappear inside the stir zone. The crack tips are marked in these figures. Note that the swept spot friction weld in fact can be considered as a small circular friction stir weld. Therefore, the shapes of two curved interfaces in Figs. 2(d) and 2(e) are different probably due to the asymmetry nature of friction stir welding.

III. EXPERIMENTS

In this investigation, alclad 2024-T3 aluminum sheets with a thickness of 1.6 mm were used. Lap-shear specimens were made by using two 25.4 mm by 101.6 mm sheets with a 25.4 mm by 25.4 mm overlap area. Two doublers were made by folding two square parts of the sheets near the ends (25.4 mm × 25.4 mm). Note that the doublers can align the applied load to avoid the initial realignment of the specimen under lap-shear loading conditions.

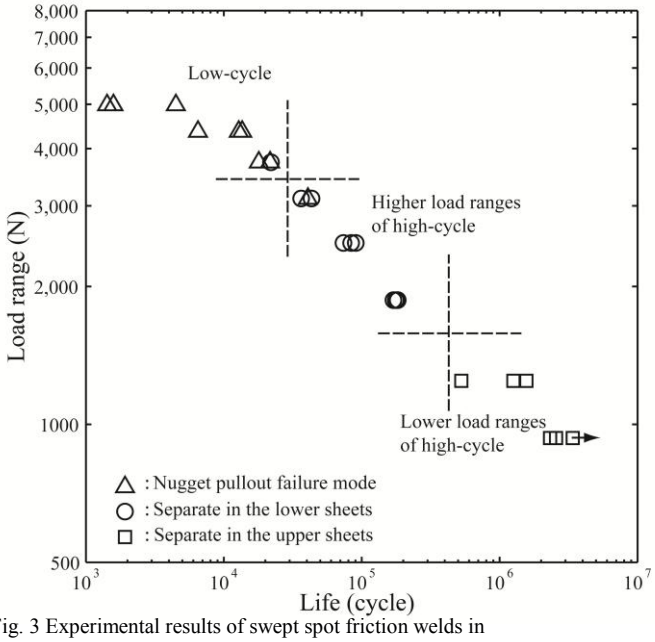

Fig. 3 Experimental results of swept spot friction welds in lap shear specimens under cyclic loading conditions.

Lap-shear specimens were first tested by using an MTS 647 testing machine at a monotonic displacement rate of 5.0 mm/min. The tests were terminated when specimens separated. The loads and displacements were simultaneously recorded during the tests. The failure loads were then used as the reference loads to determine the load ranges applied in the fatigue tests. Lap-shear specimens were then tested by using an Instron servo-hydraulic fatigue testing machine with a load ratio R of 0.1. The test frequency was 10 Hz. The tests were terminated when specimens separated, or nearly separated when the

displacement of the two grips of specimens exceeded 5 mm. Fig. 3 shows the load range as a function of the life for swept spot friction welds in lap-shear specimens under cyclic loading conditions. Due to the limited operation time of our testing machine, one test was terminated manually as the life was beyond 3.0×10^6 cycles. These results are marked by a small arrow shown in Fig. 3. Based on the experimental observation, the failure modes of swept spot friction welds in lap-shear specimens under cyclic loading conditions are quite complex. Three different failure modes can be found. In the following section, the details of the failure modes of swept spot friction welds in lap-shear specimens under different loading conditions will be presented and discussed.

IV. FAILURE MODES OF SWEPT SPOT FRICTION WELDS

We conducted experiments under quasi-static and cyclic loading conditions. Based on the experimental observation, three failure modes can be found. The failed swept spot friction welds under quasi-static loading conditions show one failure mode. The failed spot welds under cyclic loading conditions with the fatigue lives from 10^3 to 3×10^4 show a similar failure mode. The failed spot welds with the fatigue lives from 3×10^4 to 5×10^5 show another failure mode. Finally, the failed spot welds with the fatigue lives from 5×10^5 to 3×10^6 show the other failure mode. Here, we first present a two-dimensional general overview of the failure modes under loading conditions of quasi-static, low-cycle fatigue (lives of 10^3 to 3×10^4), higher load ranges of high-cycle fatigue (lives of 3×10^4 to 5×10^5), and lower load ranges of high-cycle fatigue (lives of 5×10^5 to 3×10^6).

Fig. 4(a) shows a schematic plot of the symmetry cross section of a lap-shear specimen with the sheet thickness t under an applied load (shown as the bold arrows). Fig. 4(b) shows a schematic plot of the cross section near the swept spot friction weld. In these figures, the shadow represents the stir zone, the dash line represents the un-welded interfacial surface, and the thin solid line represents either fracture surface or fatigue crack. Fig. 4(c) shows a table which lists the failure modes of swept spot friction welds under loading conditions of quasi-static, low-cycle fatigue, higher load ranges of high-cycle fatigue, and lower load ranges of high-cycle fatigue.

As shown in Fig. 4(b) and as summarized in Fig. 4(c), under quasi-static loading conditions, a necking failure is initiated at locations A and A'. The failure then propagates along the nugget circumference and finally the upper sheet is torn off. Under low-cycle loading conditions, one fatigue crack (marked by A) first emanates from the original crack tip and then another fatigue crack (marked by B) appears to emanate from the surface of the curved interface. Crack A propagates upward a bit along the interfacial surface and grows into the upper sheet thickness. Then crack A becomes crack A" that kinks a bit toward the stir zone and propagates through the upper sheet thickness. On the other hand, crack B propagates through the lower sheet thickness and then becomes a transverse crack growing toward the width direction of the specimen. Finally, only crack A propagates along the nugget circumference and the upper sheet is torn off.

Under higher load ranges of high-cycle loading conditions, the fatigue crack growth behaviors at the initial stage are similar to those under low-cycle loading conditions. However, after propagating through the upper sheet thickness, crack A becomes a circumferential crack that stops somewhere along the nugget circumference. On the other hand, crack B becomes a transverse crack growing toward the width direction of the specimen. Finally, the lower sheet is separated. Under lower load ranges of high-cycle fatigue loading conditions, the fatigue crack growth behaviors at the initial stage are also similar to those under low-cycle loading conditions. However, after propagating through the upper sheet thickness, crack A first becomes a circumferential crack that propagates partially along the nugget circumference and then becomes a transverse crack growing toward the width direction of the specimens. Finally, the upper sheet is separated. In the following, the details of the failure modes under different loading conditions will be presented by pictures and micrographs.

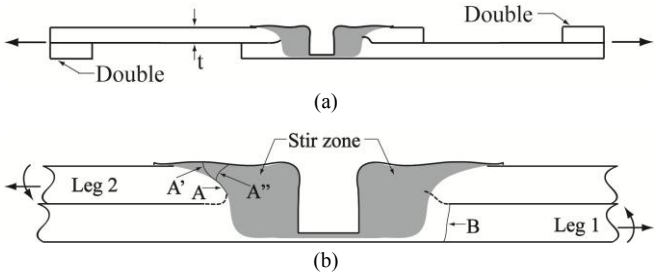

	Failure mode
Quasi-static	A → A'→ Circumferential crack → Nugget pullout
Low-cycle	A → A" → Circumferential crack → Nugget pullout
	B →Transverse through crack
Higher load ranges of high-cycle	A → A" → Circumferential crack →
	B → Transverse through crack
Lower load ranges of high-cycle	A →A" → Circumferential crack → Transverse through crack
	B →

(c)

Fig. 4 (a) A schematic plot of the symmetry cross section of a lap-shear specimen made by the concave tool with the sheet thickness t under an applied force (shown as bold arrows), (b) a schematic plot of the cross section near the swept spot friction weld, (c) the failure modes of swept spot friction welds under different loading conditions.

A. Failure Mode under Quasi-static Loading Conditions

Fig. 5(a) shows a micrograph of the symmetry cross section of a failed weld under quasi-static loading conditions. The arrows in Fig. 5(a) schematically show the direction of the applied load. The applied load stretches the upper left sheet (marked as Leg 2) and the lower right sheet (marked as Leg 1). As shown in Fig. 5(a), near the upper

left portion of the swept spot friction weld, a necking failure, marked by F2, appears from the original crack tip. Based on the experimental observation, the necking failure appears to be initiated at F2 and then propagate along the nugget circumference. Finally, the upper sheet is torn off at S1. Fig. 5(b) shows a top view of a swept spot friction weld on the lower sheet of the failed specimen. The nugget pullout failure mode can be seen.

(a)

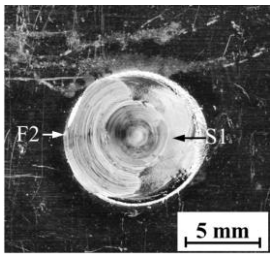

(b)

Fig. 5(a) A micrograph of the cross section of a failed swept spot friction weld under quasi-static loading conditions, (b) a top view of a swept spot friction weld on the lower sheet of a failed specimen.

B. Failure Mode under Low-Cycle Loading Conditions

Fig. 6(a) shows a micrograph of the symmetry cross section of a partially failed swept spot friction weld at the fatigue life of 2×10^3 cycles. Only one fatigue crack can be seen. Near the upper left portion of the weld, a fatigue crack (marked as crack 2) emanates from the original crack tip and grows into the upper sheet thickness. Then crack 2 kinks a bit toward the stir zone and propagates through the upper sheet thickness. Fig. 6(b) shows a micrograph of the symmetry cross section of a failed swept spot friction weld at the fatigue life of 4.5×10^3 cycles. Two fatigue cracks can be seen here. According to Fig. 6(a), after crack 2 propagates through the upper sheet thickness, the other fatigue crack (marked as crack 1) emanates from the surface of the curved interface near the lower right portion of the weld. Therefore, after propagating through the upper and lower sheet thicknesses, crack 2 appears to be the dominant kinked fatigue crack that propagates along the nugget circumference, while crack 1 becomes a transverse crack that grows toward the width direction of the specimen. Without sufficient support from the sheets near cracks 1 and 2, the nugget is rotated counterclockwise and the sheets near the nugget are therefore bent. Finally, the upper sheet is torn off at S1. Fig. 6(c) shows a top view of a swept spot friction weld on the lower sheet of a failed specimen. The nugget pullout failure mode can be seen. The large transverse crack near the right hand side of the remaining weld nugget corresponds to crack 1 in Fig. 6(b). Fig. 6(d) shows a back view of a swept spot friction weld on the lower sheet of a failed specimen. The large transverse crack near the right hand side of the remaining nugget corresponds to crack 1 in Fig. 6(b).

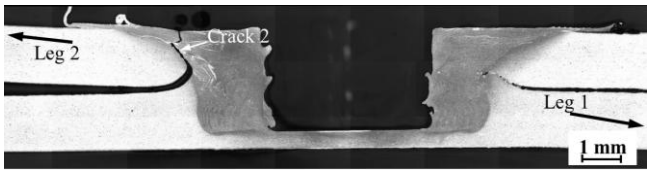

(a)

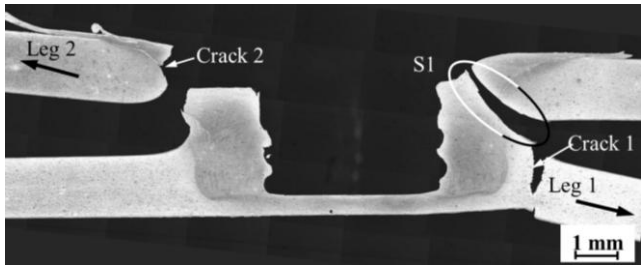

(b)

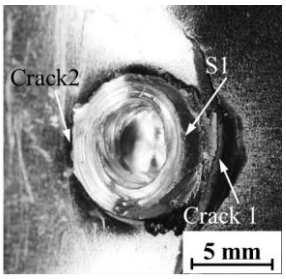

(c)

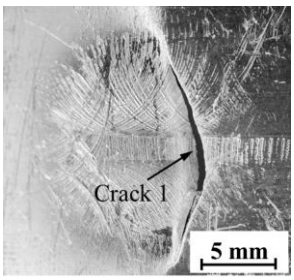

(d)

Fig. 6(a) A micrograph of the symmetry cross section of a partially failed swept spot friction weld at the fatigue life of 2×10^3 cycles, (b) A micrograph of the symmetry cross section of a failed swept spot friction weld at the fatigue life of 4.5×10^3 cycles, (c) a top view of a swept spot friction weld on the lower sheet of a failed specimen, (d) a back view of a swept spot friction weld on the lower sheet of a failed specimen.

C. Failure Mode under Higher Load Ranges of High-Cycle Loading Conditions

Fig. 7(a) shows a micrograph of the symmetry cross section of a failed swept spot friction weld at the fatigue life of 6×10^4 cycles. Two fatigue cracks can be seen. The fatigue crack growth behaviors at the initial stage are similar to those under low-cycle loading conditions in Fig. 6. As shown in Fig. 7(a), the growth rate of crack 2 appears to be faster then that of crack 1. Hence, crack 2 first propagates through the upper sheet and becomes a circumferential crack. Fig. 7(b) shows a micrograph of the symmetry cross section of a failed swept spot friction weld at the fatigue life of 9×10^4 cycles. As shown in Figs. 7(a) and 7(b), although crack 2 first propagates through the upper sheet and becomes a circumferential crack, after propagating through the upper sheet thickness, crack 2 stops somewhere in the upper sheet. On the other hand, after propagating through the lower sheet, crack 1 appears to be the dominant kinked fatigue crack that grows toward the width direction of the

specimen. Finally, the lower sheet is separated. Fig. 7(c) shows a top view of a swept spot friction weld on a failed specimen. As shown in Fig. 7(c), the small circumferential crack near the left hand side of the remaining nugget corresponds to crack 2 in Figs. 7(a) and Fig. 7(b). Fig. 7(d) shows a back view of a swept spot friction weld on a failed specimen. As shown in Fig. 7(d), the large transverse crack near the right hand side of the remaining nugget corresponds to crack 1 in Figs. 7(a) and Fig. 7(b).

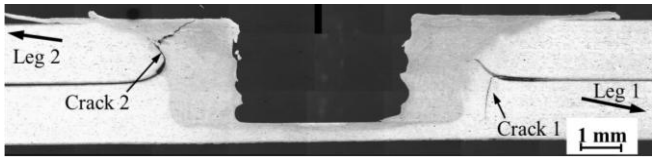

(a)

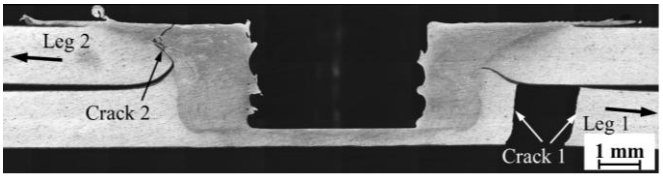

(b)

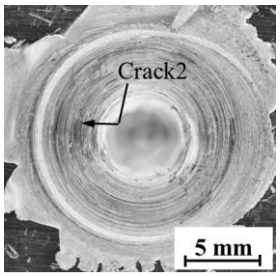

(c)

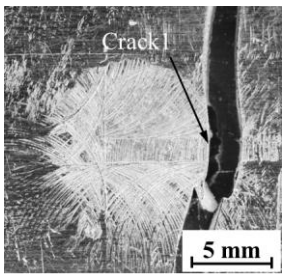

(d)

Fig. 7(a) A micrograph of the symmetry cross section of a partially failed swept spot friction weld at the fatigue life of 6×10^4 cycles, (b) A micrograph of the symmetry cross section of a failed swept spot friction weld at the fatigue life of 9×10^4 cycles, (c) a top view of a swept spot friction weld on the upper sheet of a failed specimen, (d) a back view of a swept spot friction weld on a failed specimen.

D. Failure Mode under Lower Load Ranges of High-Cycle Loading Conditions

Fig. 8(a) shows a micrograph of the symmetry cross section of a failed swept spot friction weld at the fatigue life of 10^6 cycles. Two fatigue cracks can be seen. The fatigue crack growth behaviors at the initial stage are similar to those in Fig. 7(a). As shown in Fig. 8(a), the growth rate of crack 2 appears to be faster then that of crack 1. Hence, crack 2 first propagates through the upper sheet and becomes a circumferential crack. Fig. 8(b) shows a micrograph of the symmetry cross section of a failed swept spot friction weld at the fatigue life of 1.6×10^6 cycles. As shown in Fig. 8(b), three fatigue cracks can be seen. Cracks 1a and 1b emanate from the surface of the curved interface and then stop somewhere in the lower sheet. Crack 2 appears to be the dominant kinked fatigue crack that propagates through the upper sheet thickness, grows partially along the nugget circumference, and then grows toward the width direction of the specimen. Finally, the upper sheet is separated. Fig. 8(c) shows a top view of a swept spot friction weld on a failed specimen. The large transverse crack near the left hand side of the remaining nugget corresponds to crack 2 in Figs. 8(a) and 8(b). Fig. 8(d) shows a back view of a swept spot friction weld on a failed specimen. No crack can be seen here.

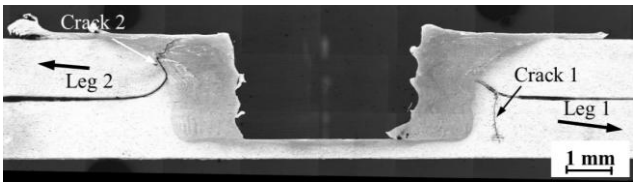

(a)

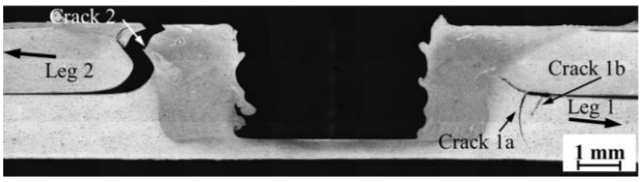

(b)

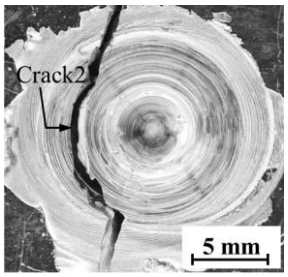

(c)

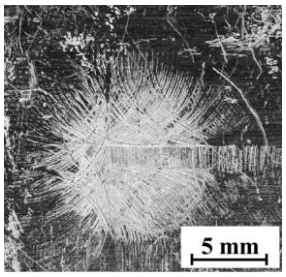

(d)

Fig. 8(a) A micrograph of the symmetry cross section of a partially failed swept spot friction weld at the fatigue life of 10^6 cycles, (b) A micrograph of the symmetry cross section of a failed swept spot friction weld at the fatigue life of 1.6×10^6 cycles, (c) a top view of a swept spot friction weld on a failed specimen, (d) a back view of a swept spot friction weld on a failed specimen.

V. CONCLUSIONS

In this paper, failure modes of swept spot friction welds made in lap-shear specimens of alclad 2024-T3 aluminum sheets are investigated based on experimental observations. Optical and scanning electron micrographs of swept spot friction welds before and after failure under quasi-static and cyclic loading conditions are examined. The micrographs show that the fracture and fatigue behaviors of swept spot friction welds under different loading conditions are quite different. Under quasi-static loading conditions, the failure mainly starts from the necking of the upper sheet near the boundary of the stir zone. Under cyclic loading conditions, two types of fatigue cracks can be found. One type initiates from the crack tip and grows into the upper sheet near the boundary of the stir zone. The other type initiates from the surface of the curved interface and grows into the lower sheet outside the stir zone. Under low-cycle and lower load ranges of high-cycle loading conditions, the dominant kinked fatigue cracks are the first type. Under higher ranges of high-cycle loading conditions, the dominant kinked

fatigue cracks are the second type. The experimental results suggest that the failure modes of swept spot friction welds under cyclic loading conditions strongly depend on the weld geometry, microstructure, and load amplitude. Note that the paths of the dominant kinked fatigue cracks can be very helpful for the fatigue life estimation of swept spot friction welds in the future study.

ACKNOWLEDGMENT

The financial support of this work by the National Science Council under Grant 96-2221-E-194-047, 97-2221-E-194-014, and 98-2221-E-194-007-MY3 is greatly appreciated.

REFERENCES

[1] P. Thornton, A. Krause, R. Davies, "Aluminum Spot Weld," *Welding Journal*, 75 (1996) 101-108.

[2] S. A. Gean, J. C. Westgate, J. C. Kucza, J. C. Ehrstorm, "Static and Fatigue Behavior of Spot-Welded 5182-0 Aluminum Alloy Sheet," *Welding Journal*, 78 (1999) 80-86.

[3] R. Sakano, K. Murakami, K. Yamashita, T. Hyoe, M. Fujimoto, M. Inuzuka, Y. Nagao, H. Kashiki, "Development of Spot FSW Robot System for Automobile Body Members," Proceedings of the 3rd International Symposium of Friction Stir Welding, Kobe, (2001) 27-28.

[4] T. Iwashita, "Method and Apparatus for Joining," US Patent 6601751 B2, (2003).

[5] G. Buffa, L. Fratini , M. Piacentini, "On the Influence of Tool Path in Friction Stir Spot Welding of Aluminum Alloys," *journal of materials processing technology*, 208 (2008) 309-317.

[6] B. Tweedy, C. Widener, J. Merry, J. Brown, D. Burford, "Factors Affecting the Properties of Swept Friction Stir Welds," SAE Technical Paper, Society of Automotive Engineers, Detroit, (2008) 14-17.

[7] J. Brown, C. Widener, G. Moore, K. Poston, D. Burford, "Evaluation of Swept Friction Stir Spot Welding in Al 2219-T6," TMS 2009 Annual Meeting, California, (2009) 215-223.

[8] J. Brown, C. Widener, D. Burford, W. Horn, G. Talia, B. Tweedy, "Corrosion and Fatigue Evaluation of Sept Friction Stir Spot Welding through Sealants and Surface Treatments," TMS 2009 Annual Meeting, California, (2009) 273-282.